ORIGINAL ARTICLE

Reconstructive

Multidetector-row Computed Tomographic Angiography in the Planning of the Local Perforator Flaps

Pavlo O. Badiul, MD, PhD*†
Sergii V. Sliesarenko, MD, PhD*†

Background: The perforator vessels are highly variable in number, localization types, hemodynamic specifications, and the anatomical interactions with other structures. For these reasons, the identification of the best perforator before the operation is very important for the choice of the main feed vessel and the design of the perforator flap.
Methods: The authors retrospectively analyzed all cases in which multiple detector computed tomography (MDCT) with 3-dimensional (3D) image reconstruction was used in the preoperative planning in preparation for the reconstruction with local perforator flaps, which took place between July 2012 and December 2014 in the hospital.
Results: A total of 24 people were examined and underwent operations with 26 reconstructions using local perforator flaps. All perforators, which were identified during the MDCT with 3D reconstruction examination, were located intraoperationally without any errors.
Conclusions: The preoperative MDCT with 3D reconstruction investigations of the topographic anatomical specifics of the perforator vessel on which the formation of the flap feed pedicle is planned allow for the fast and precise identification of the perforation at the preoperative stage while minimizing the amount of injury caused to the perforator during the operation and decrease the operation time. *(Plast Reconstr Surg Glob Open 2015;3:e516; doi: 10.1097/GOX.0000000000000496; Published online 22 September 2015.)*

The anatomy of the human vascular system has been studied for centuries. Nevertheless, questions continue to arise at each new stage in the development of surgery. The introduction of perforator flaps into the surgical practice over the last decades has expanded the reach of plastic surgery. The use of these flaps greatly simplifies the reconstruction procedures and decreases the number of surgery stages and minimizes the amount of trauma at the site of the flap harvesting. In addition, the utilization of the perforator flaps shortens the duration of operations and allows for the maintenance of the intactness of the great vessels at both the donor and the recipient sites.[1–3] However, surgery challenges remain, as the perforator vessels are highly variable in number, localization type, hemodynamic specifications, and their anatomical interactions with other structures. For these reasons,

Supplemental digital content is available for this article. Clickable URL citations appear in the text.

the identification of the best perforator before the procedure is very important for the choice of the main feed vessel and the design of the perforator flap.

In recent years, the flap design techniques have begun to incorporate the preoperative evaluation, localization, and calibration of the perforator. Such approach enables the best perforator to be selected before the dissection has begun.[4–7] Therefore, the diagnostic value of the ultrasound and radiological methods for the preoperative flap evaluations has been, lately, widely discussed in the plastic surgery community.[8–11,23]

In the last 15 years, the development of the multiple detector computed tomography (MDCT) has radically changed the way the computed tomography (CT) angiography is used for the study of the vascular pathology.[12,13] Interestingly, over the years, MDCT proved to be not only a very useful tool for the study of aorta and peripheral arteries but also a very promising noninvasive method for the localization, visualization, and characterization of the coronary artery stenosis. Moreover, MDCT allows for the investigation of the coronary vessels, the lumen diameter, and the occlusion site.[14,15] Consequently, the idea of studying the perforator vessels by MDCT has emerged as a natural extension of its current applications and as a reliable method for the precise localization of the vessels most suitable for the flap formation.[20–22]

Indeed, since 2003, MDCT has been proving itself as a highly reliable technique for the preoperative planning of Deep Inferior Epigastric Perforator (DIEP) flap for breast reconstruction. Notably, this application of MDCT has been shown to yield great results, including the significant decrease in the duration of the surgery and the amount of the postsurgical complications.[16–19] Consequently, over the past few years, a number of reports have emerged that discuss the possibility of employing MDCT for the planning of various flap types, and for the identification of perforators in various body parts, even including those that are smaller in diameter than the perforators in the front abdominal wall.[7,11] Herein, we share our experience of using MDCT with 3-dimensional (3D) visualization in the planning of the local perforator flaps in various body parts and demonstrate the effectiveness and precision of this method.

PATIENTS AND METHODS

For the purpose of this report, we have retrospectively analyzed 56 cases of reconstruction with the local perforator flaps. All procedures took place between July 2012 and December 2014 at our hospital and were performed by only 2 surgeons (P.O.B., S.V.S.) every time.

In 26 of these cases, MDCT with 3D-image reconstruction was employed in the preoperative planning and preparation for the reconstructions with the local perforator flaps. The following parameters were considered for this group: patient's age and sex, cause and area of the defect that needed reconstruction, the perforator being used, coverage of the donor site (primary close or skin graft), postsurgery complications, flap survival, and actual versus expected duration of the surgery.

The remaining 30 cases formed the control group, in which the same types of reconstructions were performed during the same period of time by the same surgeons but without the use of MDCT for procedures' preparations.

The expected duration of the procedure was calculated based on the mean time required for the control group.

Finally, the decision to use MDCT angiography was based on the consent of a patient to bear the additional financial costs of the study.

CT Scanning Technique

All perforator studies by CT angiography were carried out on 128 MDCT by a team consisting of a radiologist, a radio technician, and a plastic surgeon. During the scanning, the patients were positioned in a manner identical to their actual placement on the operating table. The patients held their breaths during the visualization of the main trunk. In addition, the scanning was limited to the segment of the body on which the surgical procedure was to be performed.

The CT angiography images were reconstructed with the help of the OsiriX (Pixmeo SARL, Bernex, Switzerland) imaging software using the techniques of maximum intensity projection and volume rendering. The so-called background structures were virtually removed during the data processing to optimize the 3D image and to enhance the visualization of small perforator vessels. The use of these formatting methods allowed for the localization of all the perforators of interest. Subsequently, the locations of the perforators discovered with the help of MDCT data were marked on the patients' skin.

In all cases, the localization of the perforators with a diameter of more than 1.0 mm was marked. In addition, the sites of the penetration of the deep fascia by perforator vessels and the directions of the perforator branches over the fascia were determined using the CT. Such treatment allowed for the creation of well-characterized flaps and provided precise information about the locations of the perfo-

Table 1. Patient Demographic Data

| Patient	Age	Sex	Diagnosis	Pedicle (Type)	Flap Size (cm)	Donor-site Coverage	Actual Time/ Theoretical Time (hours:minutes)	Complications
1	22	M	Traumatic wound of left wrist	DPAU	13×4	Primary closure + skin grafting (20 cm²)	2:15/2:35	—
2	25	M	Electric burn IV of the right hand	ARP	3×6	Skin grafting	1:50/2:35	—
3	25	M	Electric burn IV of the right hand	DPAU	3×4	Primary closure	1:00/2:35	Epidermolysis
4	46	F	Angiofibroma of left calf	PTAP	11×8	Skin grafting (150 cm²)	2:00/2:50	—
5	63	F	Liposarcoma of right calf	PTAP	11×6	Skin grafting (100 cm²)	1:30/2:50	—
6	38	M	Chronic wound of left calf	PAP	14×7	Skin grafting	1:55/2:50	—
7	38	M	Thermomechanical injury of left foot	PTAP	17×7	Skin grafting	1:55/2:50	—
8	38	M	Thermomechanical injury of left foot	PAP	15.5×7	Skin grafting	2:20/2:50	—
9	72	M	Cancer cutis of the ankle	PTAP	6×5	Skin grafting	1:50/2:50	—
10	55	F	Chronic wound of right calf	PTAP	8×9	Primary closure + skin grafting	2:00/2:50	Infection + partial necrosis
11	22	M	Traumatic wound of right heel	PAP	10×5	Skin grafting	2:00/2:50	—
12	54	F	Chronic wound in the area of left heel	PTAP	7×3	Skin grafting	1:40/2:50	—
13	46	F	Dermatofibroma of the right subclavian area	ITAP	7×13	Primary closure	2:20/3:05	—
14	49	M	Nodular melanoma of the back	LAP	17×8	Primary closure	2:30/3:05	—
15	65	M	Traumatic wound of the right Achilles	PTAP	5×3	Primary closure	2:25/2:50	—
16	35	M	Traumatic wound of the right Achilles	PTAP	6×4	Primary closure	2:00/2:50	—
17	32	F	Traumatic wound of the elbow joint	DAAP	19×5	Primary closure	2:00/2:35	Venous congestion + partial necrosis
18	52	M	Traumatic wound of the right hand	DPAU	4×12	Primary closure + skin grafting	2:10/2:35	Venous congestion + marginal necrosis
19	71	F	Contact burn of the right popliteal fossa and calf	PFAP-3	7×17	Primary closure	2:00/2:50	—
20	31	M	Scars with ulceration of the left popliteal fossa and calf	PFAP-3	4×17	Primary closure	2:00/2:50	—
21	27	M	Chronic wound of right heel	PAP	7×3	Primary closure	1:55/2:50	—
22	53	F	Scars contracture of the hand	DPAU	3×10	Primary closure	2:00/2:35	Venous congestion + partial necrosis
23	22	M	Mine fragments wound of right calf	PTAP	11×4.5	Skin grafting	2:00/2:50	—
24	22	M	Mine fragments wound of the back	DIAP	10×5	Primary closure	2:15/3:05	—
25	49	M	Mine fragments wound of the hip	LCFAP	17×8	Primary closure	2:30/3:05	—
26	25	M	Mine fragments wound of the calf	PTAP	12×5	Primary closure + skin grafting	2:00/2:50	—

ARP, artery radialis perforant; DAAP, deep artery of arm perforator; DIAP, dorsal intercostal artery perforator; DPAU, distal perforator artery ulnar; F, female; ITAP, internal thoracic artery perforant; LAP, lumbar artery perforator; LCFAP, lateral circumflex femoral artery perforator; M, male; PAP, perineal artery perforator; PFAP-3, third perforator of the profunda femoris artery; PTAP, posterior tibial artery perforator.

rators' exits and the directions of their branches on the suprafascial level.

Intraoperative Evaluation

The diagnostic data received from the MDCT technique on the predicted locations of the perforators were compared with the actual data obtained during the surgeries. The locations where the perforators actually emerged during the procedures were also marked on the patients' skin. The comparisons between the preoperative and intraoperational markings for perforators' locations were next carried out.
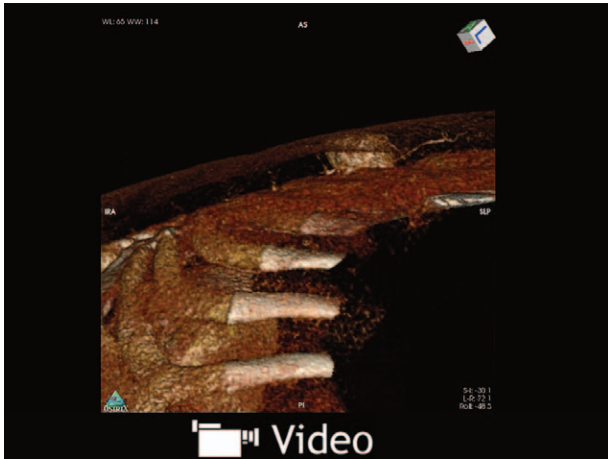
Video Graphic 1. See Video 1, Supplemental Digital Content 1, which displays MDCT angiography of the second perforator of the left internal thoracic artery. http://links.lww.com/PRSGO/XX.

RESULTS

A total of 24 people (8 women and 16 men) were examined with MDCT presurgery and then underwent 26 local perforator flap reconstruction procedures (Table 1; **See Video 1, Supplemental Digital Content 1**, which displays MDCT angiography of the second perforator of the left internal thoracic artery, http://links.lww.com/PRSGO/XX). The average patient age was 42 years (range, 22–72 years).

The areas subject to reconstruction were the thorax, small of the back, and the upper and the lower limbs. The flap pedicles included the perforators of the perineal artery (5 flaps), perforators of the arteria tibialis posterior (5 flaps), perforators of the profunda femoris artery (2 flaps), ascending skin branch of the dorsal perforator of the arteria ulnaris (4 flaps), perforator of the arteria radialis (1 flap), perforator of the deep artery of arm (1 flap), perforator of the internal thoracic artery (1 flap), and lumbar artery perforator (1 flap).

The flap size varied from 3×4 cm to 8×17 cm. The donor site was closed primarily in 13 cases, and 9 cases required skin grafting. There were complications in 5 cases: case 3—epidermolysis, case 10—marginal necrosis following infection, cases 17, 18, and 22—partial necrosis following venous congestion. In all these cases, the complications were resolved and did not significantly interfere with the treatment. The remaining 21 of the MDCT-assisted cases of the plastic surgery procedures involving the flap did not produce any complications.

All perforators identified by the MDCT examinations were located intraoperationally without any errors. The distances between the intraoperational positions of the perforators and the positions established by the MDCT analysis did not exceed 1 cm. Furthermore, there never arose the need to change the planned flap design intraoperationally. Moreover, the procedure duration of all of the MDCT-assisted cases was, on average, 28.5% shorter than that of the identical operations in the control group, which had no preoperative perforator visualization performed. The control group consisted of 30 people with the average age of 43 years (range, 22–71 years).

The average procedure duration in the control group was 2 hours 50 minutes (range, 2 hours 20 minutes to 3 hours 40 minutes).

The upper extremities surgeries lasted, on average, 2 hours 35 minutes; the lower extremities, 2 hours 50 minutes; and the trunk, 3 hours 05 minutes.

The control group had 11 cases (36%) of postsurgery complications, 3 (10%) of which were critical complications (death of the flap) (Table 1).

CASE REPORTS

Case 13

A 46-year-old woman with dermatofibroma on the right side of the subclavian area, 9×10 cm (Fig. 1).

A propeller flap on the second perforator of the internal thoracic artery was planned for the need to cover the tissue defect formed following the removal of the neoplasm.

The second perforator of the internal thoracic artery was identified and visualized using CT angiography with 3D reconstruction. The exact location where the perforator emerged and its orientation were determined precisely, which allowed for the accurate planning of the flap design (Fig. 2; **See Video 1, Supplemental Digital**
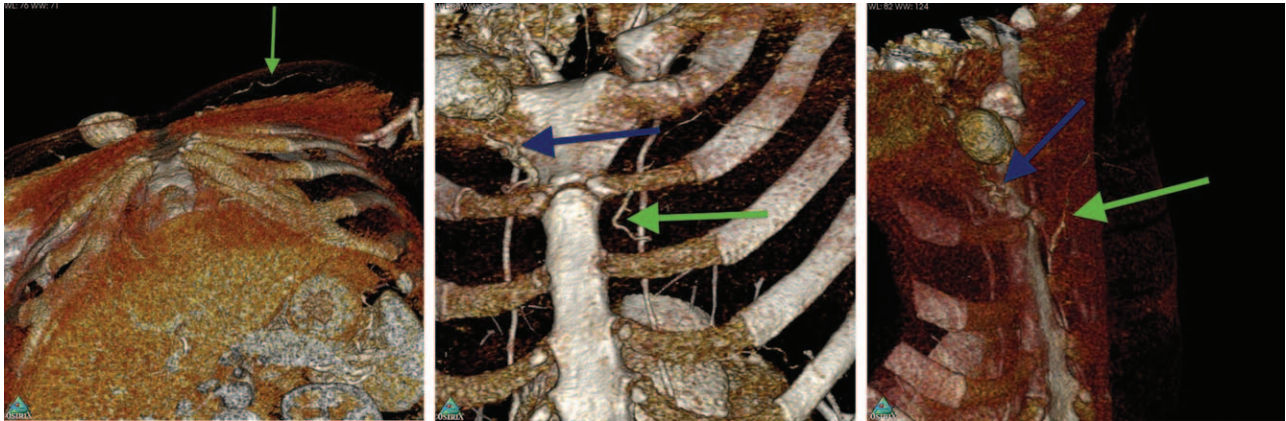

Fig. 1. Dermatofibroma in the right subclavian area and the flap design in the left subclavian area. Second perforator of the internal thoracic artery is marked.

Fig. 2. MDCT with 3D reconstruction. The green arrows points to the second perforator of the internal thoracic artery on the left. The blue arrow points to the vessel that feeds the tumor (the first perforator of the internal thoracic artery on the right).

Content 1, which displays MDCT angiography of the second perforator of the left internal thoracic artery, http://links.lww.com/PRSGO/XX).

Following the block excision of the dermatofibroma with the skin and the fascia, a circular wound emerged. The wound defect size was 11×10 cm. It was covered with an adipocutaneous flap, 7×13.5 cm in size, on the second perforator of the left internal thoracic artery, which was rotated 170° (Fig. 3). The location of the perforator, identified by CT angiography, was verified intraoperationally and found to be correct.

Case 14

A 49-year-old man with nodular melanoma on the left side of the back (Fig. 4). Plastic surgery using a propeller flap on the lumbar artery perforator was planned to cover the wound defect formed by the removal of the tumor.

During the MDCT angiography with 3D reconstruction, the lumbar artery perforators were visualized, the most suitable perforator for the flap dissection was determined, and the site of its emergence and the intra-adipose course were verified (Fig. 5; **See Video 2, Supplemental Digital Content 2**, which displays MDCT
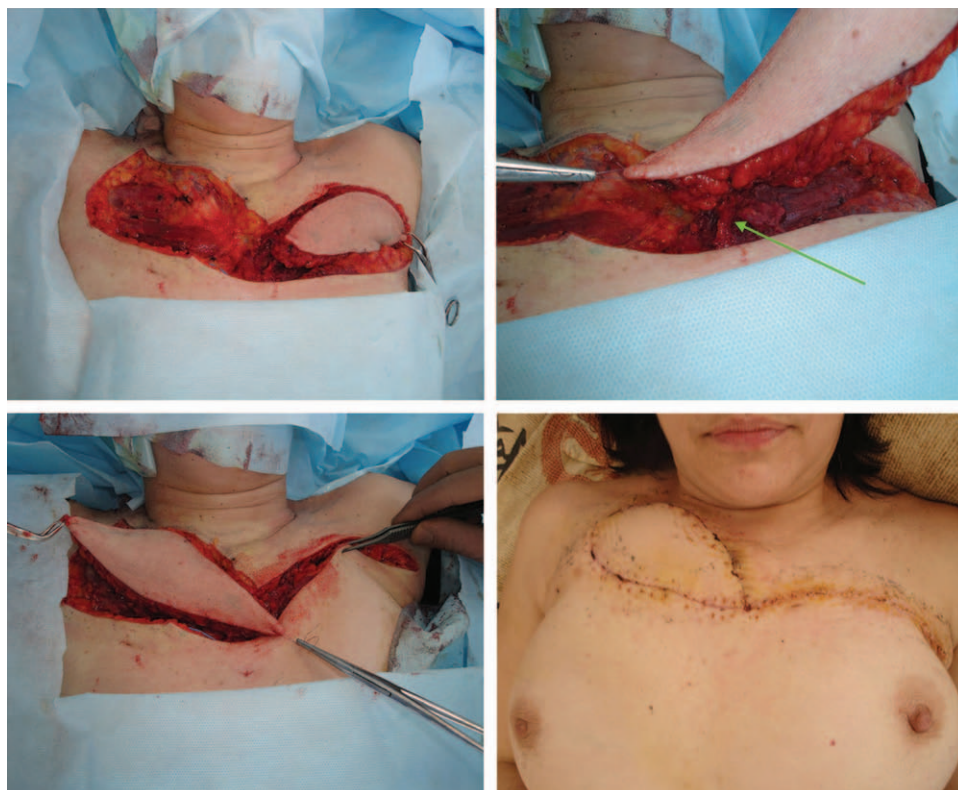

Fig. 3. A, Dermatofibroma removed. B, Flap harvested. The green arrow indicates the flap vascular pedicle. C, The flap is rotated 170°. D, The view 7 days after the surgery.

Fig. 4. Nodular melanoma of the back. The zone of removal is marked.

of the lumbar artery perforators, http://links.lww.com/PRSGO/XX).

The propeller adipocutaneous flap, 8×17 cm in size (Fig. 6), was harvested and rotated 180° to cover the wound formed following the removal of 9×12 cm melanoma.

The perforator location determined by CT angiography was verified intraoperationally and determined to be correct. The donor site underwent primary closure.

Case 15

A 65-year-old man with a sports injury (the rupture of the Achilles tendon). A wound that formed following the surgical reconstruction of the Achilles tendon would not heal for 14 months.

A distal-based sural flap was planned for the reconstruction. The perforators from the posterior tibial artery, which were saved after the primary operation, were visual-
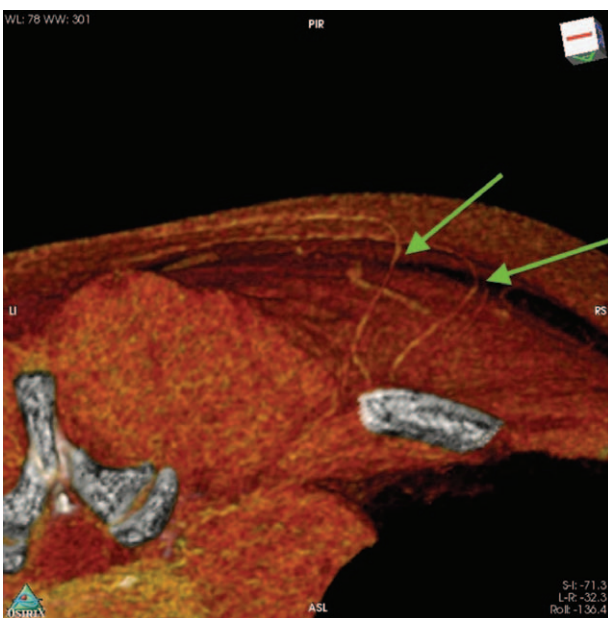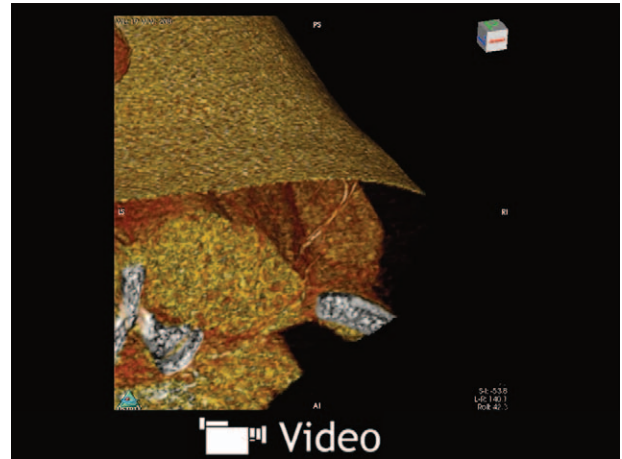

Fig. 5. MDCT with 3D reconstruction. The green arrows indicates the lumbar artery perforators.

Video Graphic 2. See Video 2, Supplemental Digital Content 2, which displays MDCT of the lumbar artery perforators. http://links.lww.com/PRSGO/XX.

ized during the MDCT angiography with 3D reconstruction. The level of the flap pedicle dissection and pivot point were also determined (Fig. 7).

A 3×5 cm fasciocutaneous flap was created and rotated 180° to cover the wound defect formed following the excision of the pathologically transformed soft tissues in the Achilles tendon area. The donor site underwent primary closure.

DISCUSSION

Employing the preoperative investigation of the topographic anatomical specifics of the perforator vessels in the planning of the flap harvesting allows for the fast and accurate perforator identification, while minimizing the amount of trauma caused to the perforator, and decreases the procedure duration.

Although the MDCT technique had been developed more than 15 years ago, the scope of its applications has been expanding over the years and has recently emerged to encompass its use as a noninvasive and a reliable tool in preoperative perforator flap analysis. As such, it enables the investigation of some rather small perforator vessels in various areas of the body. Moreover, the ability of MDCT to generate precise images of the perforator vessels in a rather short time frame makes it the most precise and comprehensive tool for producing the images of the sought perforators to date.

The first report of the application of MDCT technique to the preoperative planning of the perforator propeller flaps for closing of the defects in the various body parts was published in 2011.[11] This report described the benefits associated with the use of MDCT for locating the smaller perforators in

Fig. 6. A, Neoplasm removed. B, Flap harvested. The vascular pedicle is defined. C, Flap rotated 180°. D, The view 8 days after the operation.

various body parts, which included decreased procedure times and safer dissections. However, at that time, the authors of the study believed that MDCT was more useful for planning of the propeller flaps than for the creation of the free perforator flaps (eg, DIEP flaps).

Fig. 7. A, Posttraumatic injury in the area of the Achilles tendon. B, MDCT with 3D reconstruction. The green arrow points to the perforator from the posterior tibial artery. C, Surgery's immediate result. D, The result after 1-month treatment.

The recent improvements in the areas of data analysis and visualization by MDCT have, nevertheless, resulted in a few reports on the 3D analysis of the perforator vessels for the construction of the perforator flaps.[26,27] Here, we have demonstrated that the 3D images of the perforator vessels generated via MDCT are excellent tools in the identification of the sites where the perforators emerge as well as their locations in the soft tissues and in the suprafascial space. As such, this technique allows for an accurate investigation of the options for the flap harvesting. Overall, the preoperative flap analysis with the help of MDCT has a direct, positive effect on the operation times and on the survival of the feed pedicle and the perforator flaps.[24,25]

In general, based on the critical analysis of the literature sources and our own clinical experience, we highly recommend the use of MDCT with 3D reconstruction for the preoperative planning of the local nonfree perforator flaps in all body locations. However, we would like to note that the exceptions to our recommendation could be made for the perforator vessels of the upper extremity, in the area of the distal third of the forearm and the wrist, where the layer of the subcutaneous fat tissue is thin, potentially making the perforator visualization difficult even for the modern analytical instruments.

CONCLUSIONS

The preoperative MDCT with 3D reconstruction investigations of the topographic anatomical specifics of the perforator vessel serve as an excellent basis for the planning of the formation of the flap feed pedicle. Such presurgery activities aid in the fast and precise identification of the perforation predissection, minimize the amount of injury caused to the perforator during the operation, and reduce the operation time.

Pavlo O. Badiul, MD, PhD
53, Sergiya Nigoyana Avenue
Dnipropetrovsk 49064, Ukraine
E-mail: badyul@gmail.com

REFERENCES

1. Koshima I, Soeda S. Inferior epigastric artery skin flaps without rectus abdominis muscle. *Br J Plast Surg.* 1989;42:645–648.
2. Blondeel PN, Van Landuyt KH, Monstrey SJ, et al. The "Gent" consensus on perforator flap terminology: preliminary definitions. *Plast Reconstr Surg.* 2003;112:1378–1383; quiz 1383, 1516; discussion 1384–1387.
3. Saint-Cyr M, Schaverien MV, Rohrich RJ. Perforator flaps: history, controversies, physiology, anatomy, and use in reconstruction. *Plast Reconstr Surg.* 2009;123:132e–145e.
4. Hamdi M, Van Landuyt K, Van Hedent E, et al. Advances in autogenous breast reconstruction: the role of preoperative perforator mapping. *Ann Plast Surg.* 2007;58:18–26.
5. Phillips TJ, Stella DL, Rozen WM, et al. Abdominal wall CT angiography: a detailed account of a newly established preoperative imaging technique. *Radiology* 2008;249:32–44.
6. Rozen WM, Ashton MW, Grinsell D, et al. Establishing the case for CT angiography in the preoperative imaging of abdominal wall perforators. *Microsurgery* 2008;28:306–313.
7. Rozen WM, Paddle AM, Chubb D, et al. Guiding local perforator flaps with preoperative imaging: revealing perforator anatomy to improve flap design. *Plast Reconstr Surg.* 2012;130:130–134.
8. Gillis JA, Prasad V, Morris SF. Three-dimensional analysis of the internal mammary artery perforator flap. *Plast Reconstr Surg.* 2011;128:419e–426e.
9. Hallock GG. Doppler sonography and color duplex imaging for planning a perforator flap. *Clin Plast Surg.* 2003;30:347–357, v–vi.
10. Hallock GG. Attributes and shortcomings of acoustic Doppler sonography in identifying perforators for flaps from the lower extremity. *J Reconstr Microsurg.* 2009;25:377–381.
11. Ono S, Chung KC, Hayashi H, et al. Application of multidetector-row computed tomography in propeller flap planning. *Plast Reconstr Surg.* 2011;127:703–711.
12. Herzog C, Dogan S, Diebold T, et al. Multi-detector row CT versus coronary angiography: preoperative evaluation before totally endoscopic coronary artery bypass grafting. *Radiology* 2003;229:200–208.
13. Lawler LP, Fishman EK. Multidetector row computed tomography of the aorta and peripheral arteries. *Cardiol Clin.* 2003;21:607–629.
14. Ropers D, Baum U, Pohle K, et al. Detection of coronary artery stenoses with thin-slice multi-detector row spiral computed tomography and multiplanar reconstruction. *Circulation* 2003;107:664–666.
15. Wintersperger BJ, Nikolaou K, Becker CR. Multidetector-row CT angiography of the aorta and visceral arteries. *Semin Ultrasound CT MR.* 2004;25:25–40.
16. Masia J, Clavero JA, Larrañaga JR, et al. Multidetector-row computed tomography in the planning of abdominal perforator flaps. *J Plast Reconstr Aesthet Surg.* 2006;59:594–599.
17. Masia J, Kosutic D, Cervelli D, et al. In search of the ideal method in perforator mapping: noncontrast magnetic resonance imaging. *J Reconstr Microsurg.* 2010;26:29–35.
18. Hijjawi JB, Blondeel PN. Advancing deep inferior epigastric artery perforator flap breast reconstruction through multidetector row computed tomography: an evolution in preoperative imaging. *J Reconstr Microsurg.* 2010;26:11–20.
19. Hamdi M, Van Landuyt K, Van Hedent E, et al. Advances in autogenous breast reconstruction: the role of preoperative perforator mapping. *Ann Plast Surg.* 2007;58:18–26.
20. Imai R, Matsumura H, Tanaka K, et al. Comparison of Doppler sonography and multidetector-row computed tomography in the imaging findings of the deep inferior epigastric perforator artery. *Ann Plast Surg.* 2008;61:94–98.
21. Rozen WM, Phillips TJ, Ashton MW, et al. Preoperative imaging for DIEA perforator flaps: a comparative study of

computed tomographic angiography and Doppler ultrasound. *Plast Reconstr Surg.* 2008;121:9–16.

22. Minqiang X, Lanhua M, Jie L, et al. The value of multidetector-row CT angiography for pre-operative planning of breast reconstruction with deep inferior epigastric arterial perforator flaps. *Br J Radiol.* 2010;83:40–43.

23. Casey WJ III, Chew RT, Rebecca AM, et al. Advantages of preoperative computed tomography in deep inferior epigastric artery perforator flap breast reconstruction. *Plast Reconstr Surg.* 2009;123:1148–1155.

24. Smit JM, Dimopoulou A, Liss AG, et al. Preoperative CT angiography reduces surgery time in perforator flap reconstruction. *J Plast Reconstr Aesthet Surg.* 2009;62:1112–1117.

25. Uppal RS, Casaer B, Van Landuyt K, et al. The efficacy of preoperative mapping of perforators in reducing operative times and complications in perforator flap breast reconstruction. *J Plast Reconstr Aesthet Surg.* 2009;62:859–864.

26. Lui KW, Hu S, Ahmad N, et al. Three-dimensional angiography of the superior gluteal artery and lumbar artery perforator flap. *Plast Reconstr Surg.* 2009;123:79–86.

27. Gillis JA, Prasad V, Morris SF. Three-dimensional analysis of the internal mammary artery perforator flap. *Plast Reconstr Surg.* 2011;128:419e–426e.